

**GROWTH OF SINGLE-WALLED CARBON NANOTUBES THROUGH PEG-  
ETHANOL COLLOIDAL SOLUTION**

**By**

**SEAH CHOON MING**

**Thesis submitted in fulfillment of the requirements for the degree of**

**Master Science**

**October 2011**

## ACKNOWLEDGMENT

This thesis is the end of my journey in obtaining my Master of Science in Chemical Engineering. Throughout the journey, I have worked with a great number of peoples whose contribution deserved special mention. It is a pleasure to deliver my gratitude to them all in my humble acknowledgement.

Foremost, I would like to thank my parents and family members for their encouragement and support throughout my pursuance of master degree in Universiti Sains Malaysia (USM). Words failed me to express my appreciation to my family members. They deserve special mention for their inseparable support and persistent confidence in me.

I would like to express my sincere gratitude to my supervisor Professor Abdul Rahman Mohamed, for the continuous support of my study and research. I thank him for the unflinching support in various ways, which greatly inspire and enrich my growth as a student and researcher want to be. His patient, enthusiasm, motivation and guidance helped me in all the time of research and thesis writing.

I greatly acknowledge Dr. Chai Siang Piao for his advice, supervision, and crucial comments and suggestions, which made him a backbone of this research, and this thesis as well. His involvement with his originality has inspired and kindled me. In addition to that, I am much indebted for his valuable advice and gave his critical comment about in, which I grateful in every possible way.

During this research work, I have collaborated with many colleagues, and I wish to extend my warmest thank to all those who have helped me with my research work. Many thank to Assoc. Prof. Satoshi Ichikawa and from Osaka University, who kindly granted me his time to perform HR-TEM observation on my nanotube samples, and for answering some of my intelligent questions about the HR-TEM images captured. I also thank Professor Tadashi Itoh for giving me the opportunity to work on their HR-TEM equipment in the Institute of NanoScience Design, Osaka University. I greatly benefited from their advice, and I thank for their willingness to share their bright though with me. The visit to Osaka University was really a great and memorable experience, which was very fruitful for shaping up my ideas and research.

Special thanks to Pn. Faizah from Pusat Pengajian kaji Hayat, for their technical assistance in TEM characterization. To Mr Zuber Me and Mr Amin from SIRIM AMREC, Kulim for SEM characterization. To Mr Najib, Mr Syed and Mr Faiza from Pusat Pengajian Kejuruteraan Kimia for AFM characterization. To Cik Rohaya, thank for her technical support in Raman spectra analysis, and for her effort to create a pleasant working environment in MTDC lab. My special thanks to go to Cik Nurul, the secretary of Professor Abdul Rahman Mohamed , for helping me and assisting me in assorted ways.

I gratefully thank all the staffs of School of Chemical Engineering, USM, especially to our respected Dean, Professor Azlina Harun @ Kamaruddin and Deputy Dean, Assoc. Prof. Lee Keat Teong and Assoc. Prof. Mohamed Zailani Abu Bakar. To all administration staffs and technicians, thank you for the supports and guidance. Special thanks go to Kak Aniza, En. Syamsul Hidayat amd En. Arif for their sincere helping hand throughout my entire research activities.

Collective and individual acknowledgement are also owed to my colleagues and friends whose present in some manner perpetually refreshed, helpful and memorable. Many thanks to all my friends for their unparalleled help, kindness and moral supports towards me. I enjoyed and treasured the time we spent together and my journey will be totally different without you all. I thank everybody who was important to the successful realization of this thesis, as well as expressing my apology that I forgot to mention personally one by one.

Last but not least, the financial support provided by USM-RU-PRGS and Malaysia Technology Corporation are greatly acknowledged.

Thank you very Much!

SEAH CHOON MING

OCTOBER 2011

# TABLE OF CONTENTS

<b>ACKNOWLEDGEMENT</b>	ii
<b>TABLE OF CONTENT</b>	v
<b>LIST OF TABLES</b>	ix
<b>LIST OF FIGURES</b>	x
<b>LIST OF PLATES</b>	xv
<b>LIST ABBREVIATIONS</b>	xvi
<b>LIST OF SYMBOL</b>	xix
<b>ABSTRAK</b>	xx
<b>ABSTRACT</b>	xxii
<b>CHAPTER ONE: INTRODUCTION</b>	1
1.1 Nanotechnology	1
1.2 Carbon element	4
1.2.1 Carbon nanotubes	5
1.3 Methane	7
1.4 Spin coating	9
1.5 Problem statement	10
1.6 Objectives	12
1.7 Scope of study	13
1.8 Organization of the thesis	14
<b>CHAPTER TWO: LITERATURE REVIEW</b>	17
2.1 Single-walled carbon nanotubes	17
2.2 Synthesis of carbon nanotubes	19
2.2.1 Electric arc discharge	19
2.2.2 Laser ablation	22
2.2.3 Flame synthesis	24
2.2.4 Catalytic chemical vapor deposition	26

2.2.4.1	Plasma enhanced chemical vapor deposition	27
2.2.4.2	Hot filament chemical vapor deposition	29
2.2.4.3	Floating catalyst chemical vapor deposition	30
2.3	Catalytic chemical vapor deposition for single-walled carbon nanotubes synthesis	32
2.4	Thin film coating	35
2.4.1	Physical vapor deposition	35
2.4.2.	Solution based catalyst precursor and coating methods	38
2.5	Mechanism of Spin coating	44
2.6	Piranha solution	46
2.7	Active catalyst size control	47
2.8	Substrate and buffer layer	51
<b>CHPATER THREE: MATERIALS AND METHODS</b>		<b>55</b>
3.1	Materials and Chemicals	55
3.2	Experimental equipment and rig set-up	57
3.2.1	Spin coating unit	57
3.2.2	CNTs growth rig	59
3.2.2.1	Gas mixing section	59
3.2.2.1	Reaction section	60
3.2.2.3	Gas analysis sections	60
3.3	Experimental steps	67
3.3.1	Solution-based catalytic precursor preparation method	67
3.3.2	Silicon substrate preparation method	67
3.3.3	Catalyst deposition method	69
3.3.4	Production of CNTs by CCVD	69
3.4	Preliminary study	70
3.4.1	Preliminary study on the iron nanoparticles deposited on s silicon wafer	70

3.4.2	Preliminary test on decomposition of methane and growth of CNTs	70
3.5	Process study	71
3.5.1	Process study for the colloidal solution to form catalyst nanoparticles	71
3.5.2	Process study for spin coating to obtain uniform and small catalyst nanoparticles	72
3.5.3	Process study for the synthesis of CNTs by the CCVD	73
3.6	Characterizations	73
3.6.1	Raman spectroscopy	73
3.6.2	Scanning electron microscopy	74
3.6.3	Transmission electron microscopy/ High resolution transmission electron microscopy	74
3.6.4	Fourier transform infrared spectroscopy	75
3.6.5	Atomic force microscopy	76
<b>CHAPTER FOUR: RESULTS AND DISCUSSIONS</b>		<b>77</b>
4.1	Preliminary studies	77
4.1.1	Preliminary study on the iron nanoparticles deposited on silicon wafer	78
4.1.2	Blank test on methane decomposition and preliminary studies of catalyst nanoparticles for the synthesis of CNTs	79
4.2	Catalyst preparation studies	80
4.2.1	Process analysis of the colloidal solution	81
4.2.1.1	Formation of colloidal solution	86
4.2.1.2	Summary	88
4.2.2	Process analysis of the spin coating	89
4.2.2.1	The effect of spin speed	89
4.2.2.2	The effect of angular acceleration of spin	94

	coating and coating period	
	4.2.2.3 Summary	95
4.3	Role of piranha solution	96
4.4	Process study on CCVD	99
	4.4.1 Partial pressure of methane	100
	4.4.2 Reaction period	104
	4.4.3 Reaction temperatures	107
	4.4.4 Summary	110
4.5	Correlation between the CNTs diameter and catalyst geometric size	111
	4.5.1 Correlation between the CNT diameter and catalyst geometric size for the catalyst prepared with colloidal solution of absolute ethanol to PEG-400 at ratio 1:1 (v/v)	111
	4.5.2 Correlation between the CNT diameter and catalyst geometric size for the catalyst prepared with colloidal solution of different compositions	115
	4.5.3 Summary	117
4.6	Chemical state of the catalyst	123
	<b>CHAPTER FIVE CONCLUSION AND RECOMMENDATIONS</b>	<b>126</b>
5.1	Conclusions	126
5.2	Recommendations	128
	<b>REFERENCES</b>	<b>130</b>
	<b>LIST OF PUBLICATIONS</b>	<b>148</b>



## LIST OF TABLES

<b>Table 1.1</b>	The composition of raw natural gas	8
<b>Table 2.1</b>	Summary of researches on the CNTs growth on flat surface with solution based precursors	40
<b>Table 3.1</b>	List of chemicals and reagents	55
<b>Table 3.2</b>	Major component of the experiment rig and their function	63
<b>Table 3.3</b>	Parameters list for CCVD study	73
<b>Table 4.1</b>	Methane conversion recorded in a blank test	79

## LIST OF FIGURES

<b>Figure 1.1</b>	The diagram showing the nanotechnology region.	2
<b>Figure 1.2</b>	The allotropes of carbon: (a) diamond, (b) graphite, (c) lonsdaleite, (d,e,f) buckyballs (C <sub>60</sub> , C <sub>540</sub> , C <sub>70</sub> ), (g) amorphous carbon and (h) a carbon nanotube.	5
<b>Figure 1.3</b>	Schematic diagram of an individual carbon layer in the honeycomb graphite lattice called a graphene layer, and how it can be rolled to form a carbon nanotube.	7
<b>Figure 2.1</b>	(left) Structure of SWNTs with (a) armchair, (b) zig-zag, and (c) chiral chirality. (right) schematic 2-dimension graphene sheet vevtors a <sub>1</sub> and a <sub>2</sub> . The case where dashed line illustrate the case where zigzag (n,0) and armchair(n,n) structures, while ch with vector (4,2) is chiral structures.	18
<b>Figure 2.2</b>	HR-TEM image for SWNTs bundle.	18
<b>Figure 2.3</b>	Schematic diagram of CNT formation apparatus by the arc-discharge method.	21
<b>Figure 2.4</b>	Schematic diagram of CNT formation apparatus by the laser ablation method.	23
<b>Figure 2.5</b>	Plasma enhance chemical vapor deposition apparatus set-up.	27
<b>Figure 2.6</b>	Hot-filament chemical vapor deposition apparatus set-up.	30
<b>Figure 2.7</b>	Floating catalyst chemical vapor depositions apparatus set-up.	32
<b>Figure 2.8</b>	Schematic images for the spin coating process where (a) deposition, (b) spin up, (c) spin off and (d) evaporation stage.	44
<b>Figure 2.9</b>	A non uniform spin coating caused by high acceleration rate. Blue area denoted the coated part while white parts are non-coated.	45
<b>Figure 2.10</b>	: Schematic representation of the changes in the chemical state and the morphology of Co–Mo catalysts on quartz	49

substrates after (a) calcination and (b) reduction.

<b>Figure 2.11</b>	TEM images of the cross section of the substrates. (a) SiO <sub>2</sub> area after CVD growth. (b) Si area without any CNTs growth but precipitate with submicron-size particles near the surface. (c) Enlarged picture from the CNTs/SiO <sub>2</sub> interface in (a) showing the presence of gamma iron particles on silicon oxide surface and the growth of CNTs from the particles formed. (d) Enlarged area from (b) showing the formation FeSi <sub>2</sub> and Fe <sub>2</sub> SiO <sub>4</sub> crystals during CVD processing.	52
<b>Figure 3.1</b>	Schematic diagram of the experimental rig set-up.	62
<b>Figure 3.2</b>	Flowchart of overall research activities of this study	68
<b>Figure 4.1</b>	(a) AFM images for plain cleaned silicon wafer and (b) coated with catalyst. (Scale of the images is 1µm x 1µm)	78
<b>Figure 4.2</b>	SEM image of sparse CNTs grown on catalyst nanoparticles in the preliminary test.	80
<b>Figure 4.3</b>	AFM images showing the topography of catalyst nanoparticles prepared from colloidal solutions with (a) 0, (b) 25, (c) 50, (d) 75 and (e) 100% of absolute ethanol (scale: 1µm x 1µm).	82
<b>Figure 4.4</b>	: AFM images of the iron nanoparticles coated on silicon wafer after heat treatment and H <sub>2</sub> reduction prepared by colloidal solutions with iron nitrate concentrations of (a) 20, (b) 30, (c) 40, (d) 50, (e) 60 and (f) 70mmol/L respectively. (Size for the images is 1µm x 1µm).	84
<b>Figure 4.5</b>	(a) iron cations interact with ether oxygen in PEG, (b) PEG encapsulated iron nanocluster and anions that fill the voids in the polymer, (c) the micelles further isolate after ethanol is added. Black circle denotes iron cations nanocluster, grey circle represent anions of nitrate ions.	88
<b>Figure 4.6</b>	AFM images for the topography of catalyst spin coated with spin speeds of (a) 4000, (b) 6000, (c) 8000 and (d) 10000rpm. The colloidal solution used was 40mmol/L iron nitrate diluted in absolute ethanol and PEG-400 with	91

ratio 1/1 (v/v). (Size for the images is  $1\mu\text{m} \times 1\mu\text{m}$ ).

- Figure 4.7** AFM images showing the topography of catalyst spin coated with spin speeds of (a)4000, (b) 6000, (c) 8000 and (d)10000rpm. The colloidal solution used was 40mmol/L iron nitrate diluted in absolute ethanol and PEG-400 with ratio 1/3 (v/v). (Size for the images is  $1\mu\text{m} \times 1\mu\text{m}$ ). 92
- Figure 4.8** AFM images showing the topography of catalyst spin coated with spin speeds of (a) 6000, (b) 8000 and (c) 10000rpm. The colloidal solution used was 40mmol/L iron nitrate diluted in absolute ethanol and PEG-400 with ratio 1/3 (v/v) (size of images is  $1\mu\text{m} \times 1\mu\text{m}$ ). (d) is the SEM image for nanoparticles form when using ethanol 96% and solvent. 94
- Figure 4.9** AFM images showing the topography of catalyst spin coated (a) with ramping rate of 300 rpm/sec, spin period of 10 and (b) 50 second. (c) with ramping rate of 200 rpm/sec, spin period of 30 second. The colloidal solution used was 40 mmol/L iron nitrate diluted in absolute ethanol and PEG-400 with ratio 1/3 (v/v) (size of images is  $1\mu\text{m} \times 1\mu\text{m}$ ). 96
- Figure 4.10** FTIR spectrum of plain silicon wafer (green) and silicon wafer treated by piranha solution (red). 98
- Figure 4.11** SEM image of catalyst with 40mmol iron (III) nitrate nonahydrate in (a) pure PEG spin-coated on untreated silicon wafer and after hydrogen reduction and CVD, (b) ethanol/PEG-400, 1/1 (v/v) at the edge of untreated wafer after CVD. 99
- Figure 4.12** SEM images of carbon materials grew from methane partial pressures of (a) 0.167, (b) 0.333, (c) 0.500, (d) 0.667and (e) 1 atm and (f) HR-TEM image showing the carbon materials grown at methane partial pressure of 1 atm. 101
- Figure 4.13** Raman microscopy spectra for CNTs grown with methane partial pressure of 0.333, 0.500, 0.667 and 1.00atm. 103

<b>Figure 4.14</b>	SEM images of CNT array grown with periods of (a)5, (b)15, (c)30, (d) 45 (e) 60 minutes.	105
<b>Figure 4.15</b>	Raman microscopy spectra for CNTs with growth period 5, 15, 30, 45 and 60 minutes respectively.	107
<b>Figure 4.16</b>	SEM images of CNT array grown with growth temperature of (a) 700, (b) 850, (c) 1000 and (d) 1150 °C. (e) Low magnificant and (f) high magnificant HR-TEM image of CNTs grown at 1000 °C.	108
<b>Figure 4.17</b>	Raman spectra for CNTs grown at temperature 700, 850, 1000 and 1150 °C.	110
<b>Figure 4.18</b>	HR-TEM images showing CNTs grown from catalyst nanoparticles prepared by colloidal solutions with the iron nitrate concentration s of (a) 30, (b) 40, (c) 50, (d) 60 and (e) 70mmol/L.	113
<b>Figure 4.19</b>	Percentage of different CNTs grown from the samples by using colloidal solution with 30,40,50,60,70mm/L concentration of iron (III) nitrate as catalyst precursor.	114
<b>Figure 4.20</b>	Raman spectra for CNTs grown on flat-substrate catalysts that spin coated with colloidal solution of iron nitrate concentration of 30, 40, 50, 60 and 70mmol/L.	114
<b>Figure 4.21</b>	TEM images of CNTs grown on flat-substrate catalysts that spin coated with 40mmol iron (III) nitrate nonahydrate diluted in (a) pure PEG-400, (b) ethanol/PEG-400, 1/3 (v/v), (c) ethanol/PEG-400, 3/1 (v/v) and (d) HR-TEM image showing SWCNTs bundle grown by the catalyst prepared with the ethanol/PEG-400, 1/1(v/v).	116
<b>Figure 4.22</b>	D-band and G-band of Raman spectra for CNTs grown on flat-substrate catalysts that were spin-coated with 50mmol iron (III) nitrate nonahydrate diluted in pure PEG-400, ethanol/PEG-400, 1/3 (v/v), ethanol/PEG-400, 1/1 (v/v) and ethanol/PEG-400, 3/1 (v/v).	117
<b>Figure 4.23</b>	RBM of Raman spectra for CNTs grown on flat-substrate catalysts that spin coated with 50mmol iron (III) nitrate nonahydrate diluted in pure PEG-400, ethanol/PEG-400, 1/3 (v/v), ethanol/PEG-400, 1/1 (v/v) and ethanol/PEG-	117

400, 3/1 (v/v).

- Figure 4.24** The average geometry size of catalyst nanoparticles (red dot), mean diameter of as-grown CNTs (blue diamond) and the diameter range of the grown CNTs (vertical bar) by changing concentration of colloidal solution. 119
- Figure 4.25** The average geometry size of catalyst nanoparticles (blue square), mean diameter of as-grown CNTs (green triangle) and the diameter range of the grown CNTs (vertical bar) with ethanol/PEG-400 colloidal solutions of 0, 25, 50 and 75% ethanol. 120
- Figure 4.26** 26 (a) the carbon species decomposed on the surface of the catalyst nanoparticles and deposited to form a cap. (b) Part of the semi molten catalyst adhered to the CNTs wall and distorted the shape of catalyst due to the capillary force. (c) After the CNTs truly shaped, sudden contraction happened to the catalyst and backed to spherical shape due to surface tension of catalyst. 121
- Figure 4.27** HR-TEM image showing the CNTs grown from a catalyst nanoparticle. 121
- Figure 4.28** HR-TEM image showing the DWCNTs grown from a catalyst nanoparticle. 123
- Figure 4.29** HR-TEM image showing the catalyst encapsulated with several graphene layers. 125

## LIST OF PLATES

<b>Plate 2.1</b>	Image of the flame synthesis method, the white disc in the middle is the counterflow diffusion flame	25
<b>Plate 3.1</b>	Air compressor and vacuum pump for spin coater unit.	57
<b>Plate 3.2</b>	Spin coater unit	58
<b>Plate 3.3</b>	Experimental rig set-up	61

## LIST OF ABBREVIATIONS

AFM	Atomic force microscope
AIP	aluminium-iso-propoxide
atm	Atmospheric pressure
ATR	Attenuated Total Reflectance
C <sub>60</sub>	Buckminsterfullerene
CAGR	Compound annual growth rate
CNFs	Carbon nanofibers
CNTs	Carbon nanotubes
CVD	Chemical vapor deposition
CCVD	Catalytic chemical vapor deposition
D	Diameter
dc	Direct current
DTGS	Deuterated triglycine sulfate
DWCNTs	Double-walled Carbon nanotubes
EDX	Energy-dispersive X-ray spectroscopy
EAD	Electric arc-discharge
EIA	Energy Information Administration
FC-CVD	Floating catalyst chemical vapor deposition
FESEM	Field Emission Scanning Electron Microscopy
FePc	Iron (II) phthalocyanine
FTIR	Fourier transform infrared spectroscopy
GC	Gas chromatography
HF-CVD	Hot-filament chemical vapor deposition
HRTEM	High resolution transmission electron microscopy
I <sub>D</sub>	Intensity of D-Band
I <sub>G</sub>	Intensity of G-Band
ICT	Information and communication technology
kV	KiloVolts



L	Length
LA	Laser ablation
mm	Milimeter
mmol/L	Milimol per litre
Mo	Molybdenum
MOHE	Ministry of Higher Education
MOSTI	Ministry on Science, Technology & Innovation
MS	Molecular sieve
MS-CNCs	Multi-shelled carbon nanocapsules
MWCNTs	Multi-walled carbon nanotubes
nm	Nanometer
OD	Outer diameter
Pa	Pascal
PDMS	Poly(dimethyl)siloxane
PE-CVD	Plasma-enhanced chemical vapor deposition
PEG	Polyethylene glycol
Ph	Phosphorus
PS- <i>b</i> -PAA	Block copolymer poly(styrene- <i>block</i> -acrylic acid)
PVD	Physical vapor deposition
R&D	Research and development
RBM	Radial Breathing Modes
rf	Radio frequency
rpm	Revolution per minute
sccm	Standard cubic centimeter
sec	Second
SEM	Scanning Electron Microscope
SWCNTs	Single-walled carbon nanotubes
TCD	Thermal conductivity detector
TEM	Transmission electron microscopy
TEOS	Tetraethyl-ortho-silicate
TWCNTs	Thin-walled CNTs

$\mu\text{m}$	Micrometer
v/v	Volume/ volume
Vol%	Volume percentage
Wt%	Weight percentage
XRD	X-ray diffraction

## LIST OF SYMBOL

$\text{\AA}$

Angstrom

$\omega_{\text{RBM}}$

Wavelength of RBM

# **PENUMBUHAN NANOTIUB KARBON BERDINDING TUNGGAL MELALUI KOLOID PEG-ETHANOL**

## **ABSTRAK**

Sejak penemuan nanotub karbon (CNTs), sokongan mangkin dalam bentuk serbuk telah mendominasi bidang ini. Tetapi mangkin jenis ini mempunyai kelemahan seperti susah untuk mengkaji saiz mangkin dan memerlukan penulenan. Dalam pengkajian ini, CNTs ditumbuh dengan nanozarah ferum diatas wafer silicon melalui ferum nitrat yang dilarutkan dalam koloid polyethylene glycol (PEG) and ethanol. Ia disalut ke atas wafer silikon melalui salutan putaran and pependapan wap kimia bermangkin (CCVD) untuk sintesis CNTs. Cara ini sesuai untunk manangani masalah yang disebut. Untuk mengetahui kesan pelbagai pembolehubah proses ke atas topografi nanozarah ferum and morfologi CNTs yang ditumbuh dengan jelas, setiap pembolehubah dikaji berasingan. Pengkajian pembolehubah di selesaikan melalui tiga peringkat, termasuklah pengkajian koloid (komposisi koloid, kepekatan ferum nitrat), salutan putaran (kelajuan putaran, pecutan putaran dan masa putaran) dan CCVD (suhu tindakbalas, tekanan separa metana, dan masa tindakbalas). Ferum nitrat dengan kepekatan 40mmol/L yang dilarut di dalam koloid dengan nisbah ethanol kepada PEG 1:1 (v/v), lalu disalutkan ke atas wafer silicon dengan 8000rpm untuk 30 saat dan pecutan putaran 300rpm/sec adalah pembolehubah yang paling optimum untuk menaburkan nanozarah ferum secara sekata dan dalam size yang paling kecil di atas wafer. Sampel mangkin ini sesuai untuk menumbuh CNTs berdinding tunggal dengan selektiviti paling tinggai dan diameter yang sekata. Larutan piranha didapati berguna untuk mengurangkan

hidrofobiksite silikon oksida pada wafer. Kumpulan -OH didapati menjalin ikatan lemah dengan PEG, lalu membekalkan tenaga untuk mengurangkan ketegangan permukaan. Ini dapat menghasilkan taburan nanozarah mangkin secara sekata di atas wafer. Pada CCVD, pembolehkan operasi yang paling sesuai untuk menumbuhkan SWCNTs dengan persekataan dan selektiviti paling tinggi ialah pada 850°C, 0.333 atm tekanan separa metana dan tindakbalas untuk 30 minit. Ketiga-tiga pembolehkan ini penting untuk menumbuh SWCNTs yang mempunyai selektiviti dan kesempurnaan dinding tiub yang tinggi. Nisbah size mangkin sebelum tumbuh dengan diameter SWCNTs ialah 2.3, tetapi nisbah ini menurun ke 1.38 jika mangkin selepas tumbuh digunakan untuk dibanding. Semakin besar size purata mangkin digunakan, CNTs dengan taburan diameter yang lebih besar didapati dan juga meningkatkan nisbah di antara size mangkin dengan diameter CNTs. Akhirnya, struktur kristalografi mangkin juga dikaji. Nanozarah ferum didapati bertukar ke ferum karbid selepas pertumbuhan CNTs. Struktur kristal mangkin adalah sekata di seluruh zarah mangkin. Penguraian karbon berlaku di permukaan ferum and karbon terlarut akan resap ke tengah mangkin untuk mencapai ketepuan-super dan memulakan penukleusan CNTs. Kerja ini telah menunjukkan satu kadeah yang senang, novel and keberkesanan kos untuk mensintesis SWCNTs yang berkualiti tinggi

# **GROWTH OF SINGLE-WALLED CARBON NANOTUBES THROUGH PEG-ETHANOL COLLOIDAL SOLUTION**

## **ABSTRACT**

Since the discovery of carbon nanotubes (CNTs), powder form catalyst support becomes the dominant in this field. But powder form catalyst support possesses some shortcoming such as difficulty in catalyst size monitoring and required subsequent purification. In this study, CNTs were grown over iron nanoparticles prepared by spin coated iron nitrate that diluted in colloidal solution of absolute ethanol and polyethylene glycol (PEG). The colloidal solution was later spin coated on silicon wafer and through catalytic chemical vapor deposition (CCVD) to grow CNTs. This approach competently overcomes the shortcomings aforementioned. In order to understand the effects of various process parameters on the topography of iron nanoparticles obtained and morphology of the as-grown CNTs, all the process parameters were studied separately. The parametric study was done in three stages, representing colloidal solution (composition of colloidal solution and concentration of iron nitrate), spin coating (spin speed, angular acceleration and spin period) and CCVD (reaction temperature, methane partial pressure and reaction period) study. Iron nitrate with concentration of 40mmol/L diluted in colloidal solution at a ratio 1:1 (v/v) of absolute ethanol to PEG-400, spin coated on silicon wafer at 8000 rpm for 30 seconds and under angular acceleration of 300rpm/sec was the best parameter to distribute iron nanoparticles evenly and in small size. This catalyst sample could grow single-walled CNTs (SWCNTs) with the highest selectivity and uniformity in diameter. Piranha solution was found useful to render the hydrophobicity of silicon oxide by introducing –OH group on the wafer. The –OH group was found could form a weak bond

with PEG, providing force to reduce the surface tension. This led to the formation of catalyst nanoparticles of more uniform distribution. In CCVD, the best operating parameter to growth SWCNTs with highest uniformity and selectivity was at 850°C under methane partial pressure of 0.333atm for 30 minutes. All three parameters were crucial to synthesize SWCNTs with high selectivity and crystallinity. The ratio of pre-growth catalyst size to the SWCNTs diameter was 2.3, while the ratio decreased to 1.38 for post growth catalyst used for comparison. Bigger the average size of catalyst nanoparticle resulted CNTs with wider distribution of diameter and also higher the ratio between the average catalyst nanoparticles to CNTs diameter. Finally, the crystallographic structure of the catalyst was also demonstrated as well. The iron nanoparticle was found to be converted to iron carbide after the growth of CNTs. The crystal structure was uniform throughout the whole catalyst particles. The decomposition of carbon sources on the surface of the iron and the dissolved carbon might diffuse to the center of the catalyst to achieve supersaturation and started the nucleation of CNTs. This work has successfully demonstrated a simple, novel and cost effective route to synthesize SWCNTs with high quality.

## CHAPTER ONE

### INTRODUCTION

This chapter provides an overall introduction to the research project. A brief definition of nanotechnology and carbon nanotubes (CNTs) is outlined at the beginning chapter. Apart from the information of methane as the feedstock in this study, the brief introduction on spin coating is also given. Finally, this chapter concludes with problem statement, objectives and thesis organization of its content.

#### 1.1 Nanotechnology

Nanotechnology, also known as nanotech was first inspired by American physicist, Richard Feynman in the talk "*There's Plenty of Room at the Bottom*" at an American Physical Society meeting at Caltech on December 29, 1959 (Freyman, 1960). The term of nanotech was future evaluated by Taniguchi (1974), where "Nanotechnology mainly consists of the processing, separation, consolidation, and deformation of materials by one atom or one molecule." In 1986, a book with name *Engines of Creation: The Coming Era of Nanotechnology* was written by American engineer, Eric Drexler, who proposed the idea of a nanoscale "assembler" and popularized the concept of nanotechnology (Drexler, 1986).

Nanotechnology might be specifically defined as the design, characterization, production and application of structures, devices and systems by controlling shape and size at nanometer scale (The Royal Society & The Royal Academy of Engineering, 2004). The term of "nano", is a prefix that means "dwarf" in Greek, denotes as a billionth, while nanometer mean  $10^{-9}$  of a meter, For comparison, a



single human hair is about 80,000 nm wide, a red blood cell is approximately 5,000 nm wide and a water molecule is almost 0.3 nm across. Figure 1.1 presents the nanotechnology region.

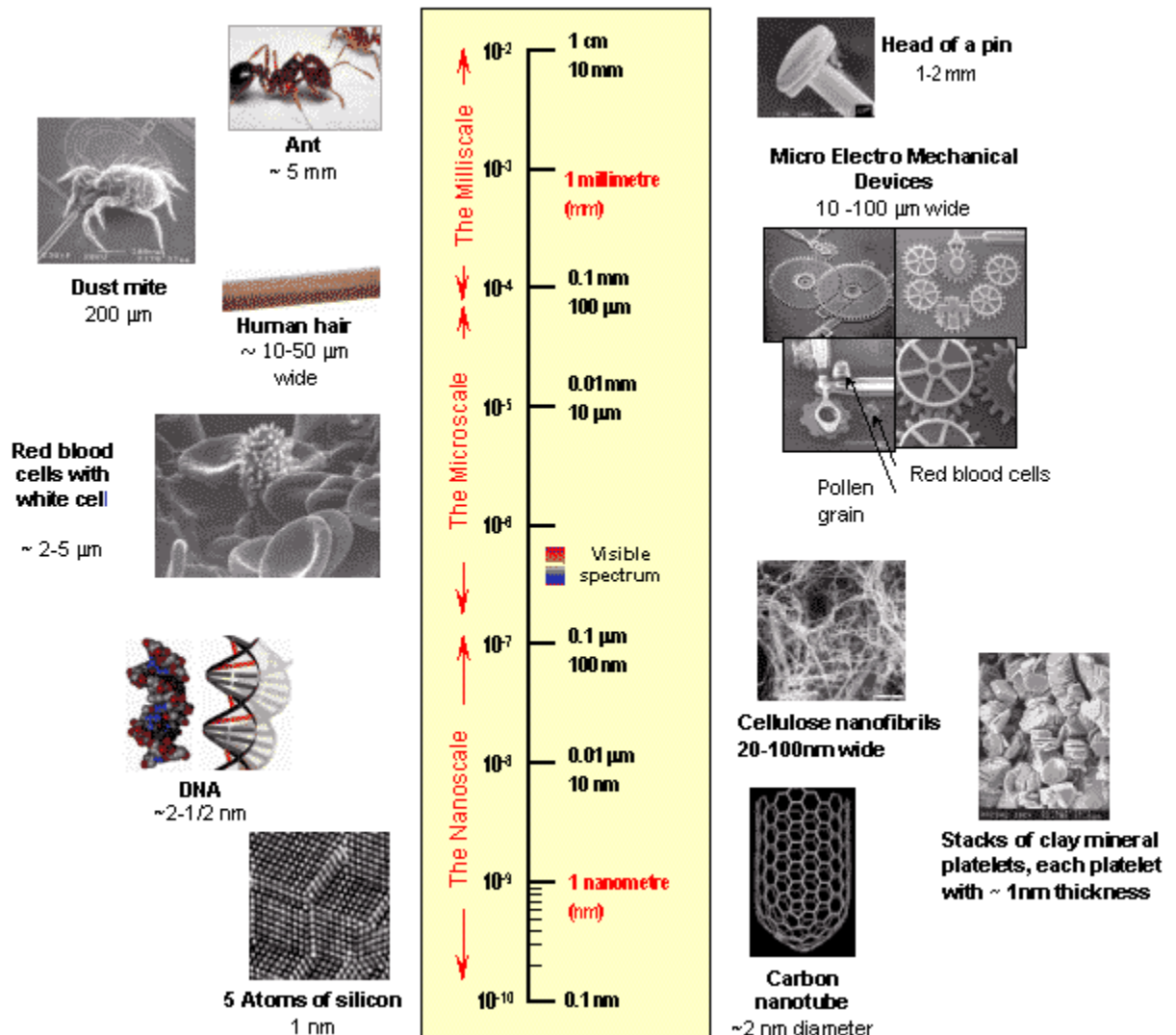


**Figure 1.1.** The diagram showing the nanotechnology region (Northwestern University, 2011)

The implications of nanotechnology are now extended from its medical, ethical, mental, legal and environmental applications, to engineering, biology, chemistry, computing, materials science, military applications, and communications. Without any doubt, nanotechnology will be the renaissance of 21<sup>st</sup> century. Nanomaterial possesses various advantages. The tininess of nanomaterials holds a

larger surface area per unit volume which makes it suitable for surface catalytic purposes. Besides, the smaller catalyst particles always possess higher catalytic activity (Hu *et al.*, 2011). Nanotechnology also brings the transistor devices into atomic scale and conducts the bloom of information and communication technology (ICT) in the early of 21<sup>st</sup> century with miniaturizes internet and multimedia-enabled devices (Bonsor and Strickland, 2011). Bioavailability was significantly improved with the imply of nanotech with a more effective drug delivery to the targeted area (LaVan *et al.*, 2003)

Nanotechnology is an expected future manufacturing technology and recognized to have the potential to revolutionize a host of industries that will make most products lighter, stronger, cleaner, less expensive and more precise. In USA alone, the government had passed the authorizations totaling US\$3.7 billions for nanotechnology R&D throughout financial year 2008 (Roco, 2006). The global market for nanotechnology incorporated in manufactured goods is projected to grow at a rate of 20% annually which worth US\$ 1.6 trillions in 2013. About 2 millions workers will involve in these industries and 6 millions will have supporting jobs (Roco, 2006).

Through MOSTI (Ministry on Science, Technology & Innovation) and MOHE (Ministry of Higher Education), the Malaysian government has funded up to RM 124.3 millions in nanotechnology area under the 9<sup>th</sup> Malaysia Plan (Economic Planning Unit, 2006). In addition, the government will set up a National Innovation Centre and a network of Center of Innovation Excellence for allowing faster commercialization and for the industry to provide fast feedback to the research work. Nanotechnology has now been included as one of the growth engines for the new

economic policy, as announced by the prime minister of Malaysia, Datuk Seri Najib Tun Razak, on a separate occasion. (Jiang, 2009).

## 1.2 Carbon element

Carbon can be found in many different compounds, it is the sixth most abundant element in the universe and the name "carbon" comes from Latin, *carbo*, with the same meaning. Inside carbon atom, 2 electrons are found in the 1s orbital close to the nucleus. The next two will go into the 2s orbital. The remaining will be in two separate 2p orbitals which having the same energy level. This configuration can be further hybridized to the  $sp^3$  configuration ( $2s^1 2p_x^1 2p_y^1 2p_z^1$ ) to form tetrahedral coordinated carbon such as methane and diamond. Meanwhile for certain carbon allotropes such as graphite, graphene and carbon nanotubes, the carbon atom undergoes  $sp^2$  hybridization. In  $sp^2$  hybridization, one s-orbital and two p-orbitals undergo hybridization, leaving another p-orbital unaffected. The remaining p-orbital is forming the distributed pi-bonds that reside above and below each graphite sheet. This delocalized pi system is responsible for the electrical conductivity of graphite. In the meantime, the other electrons in  $sp^2$  hybrid orbital forming strong covalent bond with each other and provide a magnificent mechanical strength for those materials. Figure 1.2 shows the allotropes of carbon.

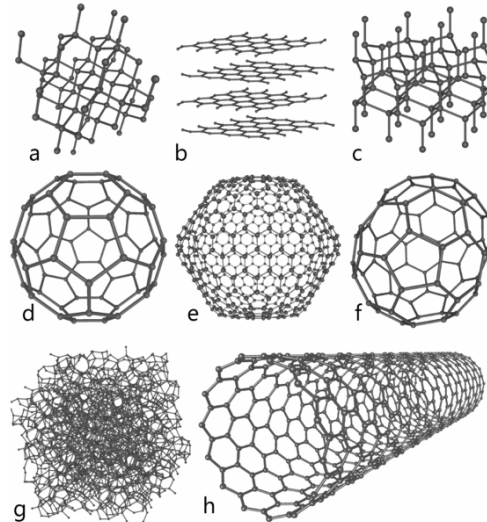


**Figure 1.2.** The allotropes of carbon: (a) diamond, (b) graphite, (c) lonsdaleite, (d,e,f) buckyballs (C<sub>60</sub>, C<sub>540</sub>, C<sub>70</sub>), (g) amorphous carbon and (h) a carbon nanotube ( Giorcelli, 2008).

### 1.2.1 Carbon nanotubes

The discovery of buckminsterfullerene (C<sub>60</sub>) (Figure 1.2 (d)) in 1985 had led to an entirely new branch of carbon chemistry (Kroto *et al.*, 1985). CNTs (Figure 1.2 (h)) was first observed by Iijima in 1991, from direct current arching of graphite for preparation on fullerenes using transmission electron microscopy (TEM) (Iijima, 1991). Two years later, single-walled carbon nanotubes (SWCNTs) were synthesized by Iijima and Ichihashi (1993) and Bethune *et al.* (1993). The research on CNTs subsequently began in earnest worldwide. However, the earliest CNTs was believed to be found in Damascus blade made in 17<sup>th</sup> century, and it is believed the use of CNTs was as early as 8<sup>th</sup> century where the first Damascus blade was made (Inman, 2006).

CNTs can be described as a sheet of honeycomb graphite lattice called graphene that rolled into a cylinder with nanoscale hollow tubular structure. The diameter of CNTs is in order of few nanometer while their length can be up micrometer range, the longest CNT recorded is 18.5 cm (Wang *et al.*, 2009). CNTs

are strongly related to 3-D-graphite when considering their large curvature as shown in Figure 1.3. CNT structures are constructed by carbon with C6 ring fusions and also C5 ring fusions so that cylinders curvatures can be formed (Kulkarni and Khot, 2010). SWCNT is the CNTs that form with one-atom-thick layer of graphene sheet that rolled into a seamless cylinder. The diameter of SWCNTs is normally close to 1nm. Meanwhile, multi-walled carbon nanotubes (MWCNTs) formed with multiple rolled layers (concentric tubes) of graphite. The inter-layer spacing is 0.34 nm, which corresponds to the inter-layer distance of 0.35 nm in graphite (Dresselhaus et al, 2001). The diameter of the MWCNTs can achieve up to hundred nanometers (Meyyappan, 2005).

CNTs are the major branch of nanotechnology field which experiences substantial progress for both understanding the fundamental properties and the characterization of its structure since discovered by Iijima (1991). Exploring in possible engineering applications also come into full swing and being applied in the areas of electronic, energy storage, drug delivery, catalysis, nanocomposite, hydrogen storage and etc. The global market for CNTs was worth US\$50.9 millions by the end of 2006 and had reached US\$79.1 millions by 2007. At a compound annual growth rate (CAGR) of 73.8%, this booming market will reach US\$807.3 millions by 2011 (Report Linker, 2004). CNTs is a field that having a great potential in near future.

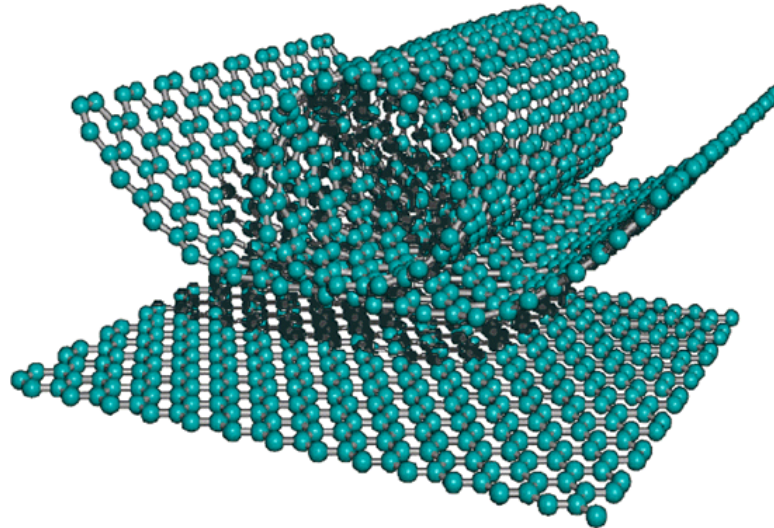


**Figure 1.3.** Schematic diagram of an individual carbon layer in the honeycomb graphite lattice called a graphene layer, and how it can be rolled to form a carbon nanotube. (Endo et al 2004)

### 1.3 Methane

Methane is a colorless, odorless gas with a wide distribution in nature with chemical formula  $\text{CH}_4$ . It has a high global warming potential of 72 as compare with carbon dioxide with 25 (Foster and Ramasamy, 2007). The major source of methane is come from natural gas reservoir underground. Alternative sources of methane including biogas are generated by the fermentation of organic matter such manure, wastewater sludge, municipal solid waste or biodegradable feedstock under anaerobic condition. The world reserve of natural gas was estimated at 6,609 trillions cubic feet at 2010 (EIA, 2010). Malaysia is a net exporter for natural gas having 83.0 trillions cubic feet of proven natural gas reserves and ranks 14<sup>th</sup> in the world (Ali and Khan, 2010). From Table 1.1, the raw natural gas in Malaysia with relatively high composition of methane and relatively clean, due to low hydrogen sulfide composition, a source for  $\text{SO}_x$ .

**Table 1.1.** The composition of raw natural gas (Natural Gas 2011, Gas Malaysia, 2011)

composition	formula	Typical natural gas	Malaysia	natural gas
Methane	CH <sub>4</sub>	70-90%		92.73%
Ethane	C <sub>2</sub> H <sub>6</sub>			4.07%
Propane	C <sub>3</sub> H <sub>8</sub>	} 0-20%		0.77%
Butane	C <sub>4</sub> H <sub>10</sub>			0.14%
Carbon dioxide	CO <sub>2</sub>	0-8 %		1.83%
Oxygen	O <sub>2</sub>	0-0.2%		Trace
Nitrogen	N <sub>2</sub>	0-5%		0.45%
Hydrogen sulfide	H <sub>2</sub> S	0-5%		trace
Rare gas	Ar, He, Ne, Xe	trace		trace
Other hydrocarbon		trace		trace

In the industrial sector, methane is often used as a raw material for products such as hydrogen, fertilizer and plastic. It is also commonly used as an energy source. Now, the utilization of methane can be extended to CNTs and carbon nanofibers (CNFs) which are more valuable product. Methane decomposes to carbon radical and hydrogen with catalyst and high temperature. The carbon later dissolves into catalyst and form CNTs or CNFs. Meanwhile, hydrogen will be the side product for the reaction. Because of the reaction takes place in inert condition, the hydrogen produces is CO<sub>x</sub>-free, which is a suitable fuel for fuel cells and methanol production.

## **1.4 Spin coating**

Spin coating is a method that used to apply uniform thin film to flat substrate. Normally, a solution puddle is placed on the center of the substrate which is the axis of rotation. It's then rotated at very high speed to spin away the excess amount of solution by centrifugal force. The inertia of solution is the reason solution ejected radially outward (Norrman, 2005, Lawrence, 1988). A thin film will form on the surface of substrate as a result of surface interaction. The thickness of the film is determined by the centrifugal force from the spin speed and the fluid viscosity. Meanwhile the uniformity is determined by solvent viscosity and the surface interaction between resin material, substrates and fluid (Lawrence, 1988). Since the resin begins to dry during the first part of the spin cycle, acceleration need to accurately controlled, spin time and exhaust for fume also affect the coating.

The advantage of spin coating is repeatability of the results with easy operation. However, subtle variation in the parameters in the spin process can result in drastic variations in the coated film. Besides, there are also other shortcomings in spin coating, such as the surface tension effect of the fluid will oppose the uniformity and topography of coating for non volatile fluid (Hart *et al.*, 2006). On the other hand, the high evaporation rate of volatile fluid will also deteriorate the uniformity of the resulted coating.

## **1.5 Problem statement**

It is already two decades that CNTs were discovered. Various techniques and improvements have been developed either for the development of catalyst or the CNTs synthesis process. Common methods that been used for the CNTs production are electric arc-discharge (EAD), laser ablation (LA), flame synthesis and catalytic



chemical vapor deposition (CCVD). Among, CCVD is the most common approach that has been studied by the researchers around the world. The most attractive part of CCVD is its simplicity and low operating cost. CCVD also can be upgraded to large scale production with proper modification. CNTs with various morphology and structure, such as MWCNTs, SWCNTs, Y-junction CNTs, carbon nanofiber (CNFs), bamboo-structured CNTs, herring boned-liked structure and CNTs with various diameters can be synthesized through CCVD by controlling the operating parameters and the catalyst used.

SWCNTs can be grown from CCVD with proper catalyst and operating parameters control, which exhibit electrical properties that are not shared by the MWCNTs and make SWCNTs suitable in the application of nanoelectronics such as electrochemical capacitors (Liu *et al.*, 2006a), field effect transistor (Liu *et al.*, 2010) and probe electrode for DNA (Zhang and Jiao, 2009). The diameter of the SWCNTs is important in microelectronic industry because the electrical and optical properties of SWCNTs are strongly dependent upon their diameter (Hasegawa and Noda). The synthesis of SWCNTs is a complex process, and the complexity further increase for synthesizing CNTs in a precise diameter range.

Conventional SWCNTs are synthesized using catalyst in powder form, where active catalyst is impregnated onto the support. The drawback of this method is the harshness for the active catalyst size monitoring. This will cause the precise control of the catalyst nanoparticles distribution become difficult. Normally, concentrated acid, high temperature and vigorous stirring are essential in the purification process. These will cause certain degree of destruction on the wall structure of CNTs. As a result, flat surface substrate is utilized to overcome this problem. The size of catalyst can be easily observed through Scanning Electron Microscope (SEM). Furthermore, the

coated catalyst nanoparticles are firmly deposited on the substrate. The grown CNTs can be easily removed by razor blade if the CNT array is thick enough, or by simple sonication in organic solvent. If the distribution of the catalyst is dense enough, aligned CNTs can also be synthesized.

Catalyst is playing the most important role for growing CNTs. Two major approaches are widely used for the catalyst coating on the flat substrate. Physical vapor deposition (PVD) is the most common and most mature method. PVD is a high vacuum process which vaporizes the bulk catalyst by a physical mean and deposit on the substrate in nanoparticles form. It is an expensive method where sophisticated apparatus is necessary, such as vacuum chamber and magnetron sputtering cathode, addition of high vacuum and high temperature further increase the operating cost. Since 2003, researchers start to search for other coating method for catalyst deposition. After since, solution based catalyst precursor has been developed. Dip-coating (Murakami *et al.*, 2003a, Murakami *et al.*, 2003b), spray coating (Terrado *et al.*), spin coating (Chaisitsak *et al.*, 2004, Kim *et al.*, 2005) and microcontact printing (Quist *et al.*, 2005) have been used to obtain a thin film of catalyst solution on substrate. However, the study of these approaches still remain rare, especially in SWCNT synthesis. To date, various solutions such as colloidal solution, magnetic fluid and *etc* have been used as the dispersion solution for the catalyst particles and CNTs with different morphology could be synthesized. However, SWCNTs are only reported on the catalyst which utilizes the chemical state changing of catalyst with the aiding of other non-active metal (Murakami *et al.*, 2003a). Size control with physical mean only reported once for the SWCNTs and the selectivity is low and mixed with other forms of CNTs. (Chaisitsak *et al.*, 2004).

After summarizing the problems faced in SWCNTs synthesis, a new colloidal solution based on polyethylene glycol (PEG) and absolute ethanol is developed to disperse iron nanoparticles evenly and desired size on silicon wafer for SWCNTs synthesis. It is followed by the study of various parameters in spin coating to control the iron nanoparticles size on silicon wafer. Lastly, the catalyst coated wafer goes through simple CCVD for decomposition of methane for the production of SWCNTs and hydrogen as a side product.

## **1.6 Objectives**

The present study has the following objectives:

1. To study the mechanism of formation of colloidal solution at different percentages of PEG and absolute ethanol to obtain uniform and nanoscale iron nanoparticles distribution.
2. To study the effect of spin coating parameters on SWCNTs yield and characteristic, and to determine the decisive process variables on the uniformity and size distribution of iron nanoparticles on silicon wafer.
3. To examine the various process parameters in catalytic chemical vapor deposition on the topography and morphology of the MWCNTs and SWCNTs produced.
4. To investigate the structural, morphology and diameter of as-grown SWCNTs by performing various characterization techniques.

## 1.7 Scope of study

This research consists of 3 major studies (i) development of a new colloidal solution which composed with PEG and absolute ethanol at different compositions. The study was carried out following the mechanism of the micelles formation that isolated the iron nanoparticles in the colloidal solution; (ii) Pretreatment of silicon wafer to enhance the surface interaction between colloidal solution and wafer. The spin coating parameters was studied to determine the decisive process variables on the uniformity and desired size distribution of iron nanoparticles on silicon wafer; (iii) CCVD of methane was performed to study the operating parameters on the morphology of the as-grown MWCNTs and SWCNTs. The effluent gases were analyzed using on-line gas chromatography (GC). The topography of iron coated silicon wafer was analyzed through SEM and atomic force microscope (AFM). The treated silicon wafer and colloidal solution were characterized by Fourier transform infrared spectroscopy (FTIR) to study its functional group. The produced CNTs were characterized using SEM, transmission electron microscope (TEM), high resolution TEM (HR-TEM) and Raman spectroscopy.

Firstly, a preliminary test was carried out to examine the suitability of PEG-ethanol colloidal solution to obtain catalyst nanoclusters and nanoparticles after coated on the substrate. Initially, the iron nitrate was diluted in the colloidal solution and then spin coated on silicon wafer. The colloidal solution coated wafer was thermally treated to obtain catalyst nanoparticles onto the wafer. Later on, another preliminary test was conducted to determine the suitability of horizontal quartz tube reactor for methane decomposition. The test study was conducted with plain silicon wafer, followed by catalyst deposited wafer. The objective of this test was to determine the capability of the catalyst nanoparticles to decompose methane in

horizontal quartz tube reactor and also to ensure the materials of reactor is suitable at the reaction temperature. Next, colloidal solution and spin coating parameters were studied to obtain the catalyst nanoparticles that distributed evenly, uniformly and with desired size on the wafer. The catalyst nanoparticles that most likely to form SWCNTs was selected for the reaction process study to determine the decisive variables for the morphology of the as-grown CNTs. Besides that, the importance of silicon wafer pretreatment and the mechanism of for the formation of colloidal solution was also investigated.

Then, the research work was followed by the investigation of the correlation with the size of pre-growth catalyst nanoparticles and as-grown CNTs diameter. Last but not least, the chemical state of the catalyst was also studied.

## **1.8 Organization of the thesis**

This thesis consists five chapters. Chapter One (Introduction) is giving an outline of the present research, including the brief introduction of nanotechnology and CNTs, followed by the information of methane, spin coating and hydrogen. Problem statement is then defined after reviewing the existing limitations faced in the synthesis of SWCNTs. Hence, a relatively new approach is designed to overcome the limitations. The objectives of present work are carefully set with the goal to solve the problems faces. Next, the scope of study given and organization of the thesis highlights the content and arrangement of each chapter.

Chapter Two (Literature Review) summarizes the past research work related to this area and their findings. It starts with the brief introduction of SWCNTs, followed by existing method for CNT synthesis, process variables of CCVD and its influence on SWCNTs synthesis. Next, the thin film coating methods such as physical

vapor deposition and solution based precursors with coating methods are reviewed to investigate the advantages and disadvantages of each method. It is followed by the review on the spin coating mechanism and piranha solution. Also included is the summary function of substrate and buffer layer.

Chapter Three (Materials and Methods) discusses the experimental materials and research methodology for present work. This chapter describes the detailed information on the overall flow of this research and experimental methods applied in this research. The detailed information of materials and chemicals used are listed as well. The analytical techniques end up this chapter.

Chapter Four (Results and Discussions) is the most important part of this thesis. It includes all the data and findings of present work. This chapter includes preliminary study, colloidal solution and spin coating study, role of piranha solution, CCVD process parameters study, correlation between catalyst size to CNTs diameter and chemical state study on catalyst.

Chapter Five (Conclusions and Recommendations) summarizes the results obtained in the present research. It includes the overall research findings and some concluding remarks. Later on, suggestions are given to improve the present study and future study to be conducted is being proposed. These recommendations and suggestions given after considering the significant findings, the conclusions as well as the limitations and difficulties encountered in the present work.

## CHAPTER TWO

### LITERATURE REVIEW

#### 2.1 Single walled carbon nanotubes

Single-walled carbon nanotubes (SWCNTs) are an important variety of CNTs because they exhibit unique electric properties. Their electrical conductivity can show metallic or semiconducting behavior. Electronic band structure calculation can predict that the  $(n,m)$  indices determine the metallic or semiconducting behavior of SWCNTs. The integers  $n$  and  $m$  denote the figure of unit vectors along two directions in the honeycomb lattice of graphene which determine the chirality of SWCNTs. If  $m = 0$ , the nanotubes are called zigzag (Figure 2.1). If  $n = m$ , the nanotubes are called armchair (Figure 2.1 (a)), Otherwise, they are called chiral (Figure 2.1(d)) (Mintmire *et al.*, 1992, Saito *et al.*, 1992, Odom *et al.*, 1998). A SWCNT is considered metallic if the value  $n-m$  is divisible by three. Otherwise, the nanotube is semi-conducting. The close packing arrangement of SWCNT in bundles due to van der Waals interactions is also demonstrated in Figure 2.2. The packing can be observed as a diamond lattice or hexagonal close packing.

The physical properties of SWCNTs have made them an extremely attractive material for the manufacturing of nano devices. A SWCNT can be up to 100 times stronger than that of steel with the same weight. The Young's Modulus of SWCNT is up to 1TPa, which is 5 times greater than steel (230 GPa) while the density is only 1.3 g/cm<sup>3</sup>

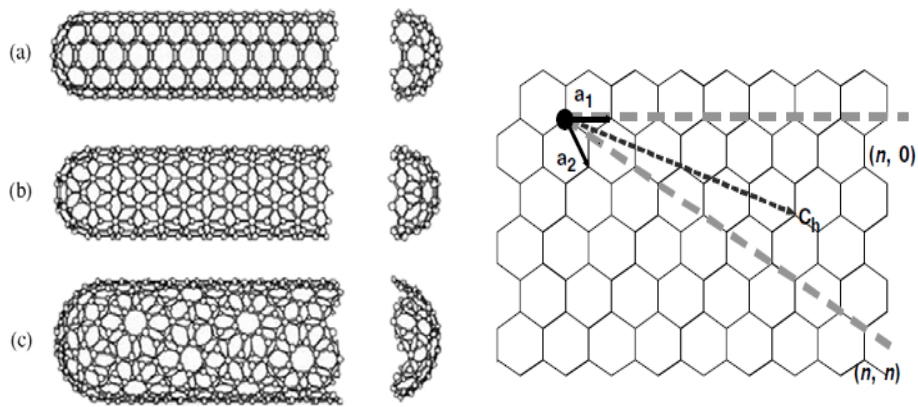


**Figure 2.1.** (left) Structure of SWNTs with (a) armchair, (b) zig-zag, and (c) chiral chirality. (right) schematic 2-dimension graphene sheet vectors  $a_1$  and  $a_2$ . The case where dashed line illustrate the case where zigzag ( $n,0$ ) and armchair ( $n,n$ ) structures, while with vector  $(4,2)$  is chiral structures. (Odom *et al.*, 1998)



**Figure 2.2.** HR-TEM image for SWNT bundle

and the thermal conductivity (2000 W/m.K) is five times greater than that of copper (400 W/m.K) (Terrones, 2003, Hone *et al.*, 1999). SWCNTs may take advantage on



properties that are normally associated with molecular species, such as solubility in organic solvents, solution based chemical transformations, chromatography, spectroscopy, which suitable for various applications (Niyogi *et al.*, 2002). The high surface area of SWCNTs makes them suitable for gas storage, such as hydrogen (Cao *et al.*, 2001). Meanwhile the strong and stable carbon-carbon bonding and hollow tube structure with diameter range of 1-2 nm enable SWCNTs for use in nanoscale test tube (Borowiak-Palen, 2007) and also membrane for gas separation (Mi *et al.*, 2007)

## **2.2 Synthesis of carbon nanotubes**

Since ever the first CNTs synthesized in 1991 in sophisticated mean, the research on the growth of CNTs has been brought into full swing all over the world. After 2 decades of the evolution, various approaches had been developed in order to control the structure and morphology of the as-grown CNTs and bring the synthesis to energy efficient and simpler means. In general, there are 4 major approaches that widely studied in the synthesis of CNTs, namely electric arc discharge (EAD), laser ablation (LA), flame synthesis and catalytic chemical vapor deposition (CCVD). All these methods will be discussed in this section.

### **2.2.1 Electric arc discharge**

Electric arc discharge is the first technique been used to study the growth of CNTs by the Iijima (1991). However, it was first used for the synthesis of fullerenes. In fact, EAD was later developed for the production of both MWCNTs and SWCNTs. In EAD, an arc is struck between two graphite electrodes in a inert gas atmosphere to synthesize long and straight MWCNTs that closed at both ends (Iijima and Ichihashi,

1993) and Bethune *et al.* (1993) reported that an arc discharge by using a cathode that with metal catalysts (such as cobalt, iron or nickel) mixed to graphite powder may results a deposit containing SWCNTs. Gram-scale of the CNTs production has also been demonstrated by Ebbesen and Ajayan (1992).

The EAD is usually carried out in an evacuated reactor with inert gas at low pressure. The electron arc is stabilized at this atmosphere and boost the sublimation of carbon atoms from the electrode for the CNTs formation in the deposition process (Vittori Antisari *et al.*, 2003) as shown in Figure 2.3. The ambient gas that first used was inert gas such as He and Ar, but the CNTs with the best crystallinity was found in CH<sub>4</sub> or H<sub>2</sub> (Zhao *et al.*, 1997), assisted by the high temperature and high activity of the hydrogen arc. Meanwhile, a voltage in the range of a few tens of volts and direct current of 50 to 100 A is normally applied between two graphite electrodes to produce high temperature. According to Ajayan and Ebbesen (1997), the best operating conditions of EAD to synthesis MWCNTs was 20 V of potential different, current density of 50 Acm<sup>-1</sup> and gas pressure of 500 Torr with inter electrode distance of 1 mm. The growth rate of CNTs is proportional to the electric current applied. However, higher current resulted more catalyst been attracted to the cathode, and less on released for the nucleation of CNTs. Furthermore, amorphous carbon was favorable due to evaporation of carbon cluster instead of carbon nanoparticles (He *et al.*, 2007). The growth temperature is partially influenced by the current, higher temperature always resulting CNTs with larger diameter (Liu *et al.*, 2004).

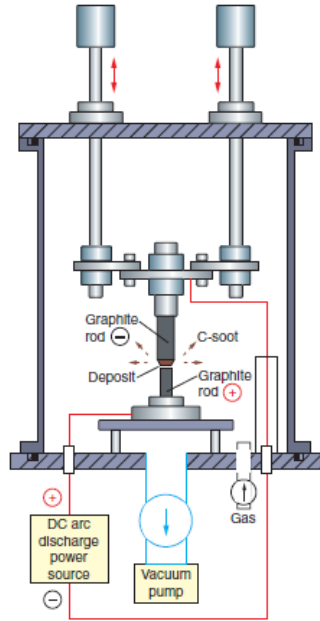


**Figure 2.3.** Schematic diagram of CNT formation apparatus by the arc-discharge method (Ando *et al.*, 2004)

EAD always requires a vacuum equipment, reacted gases, a high temperature furnace along with a heat exchange system. To overcome the complexity and expensive machinery, a much cheaper and simple liquid environment EAD was developed. Liquid nitrogen was used to replace the inert gas and it was found better in maintaining the temperature gradient within the plasma and well as protective agent for the as-grown CNTs (Ishigami *et al.*, 2000). De-ionized water was also used to perform EAD to further simplify the method and the CNTs were found better in yield (Hsin *et al.*, 2001). In liquid nitrogen EAD, the strong evaporation of liquid nitrogen and extreme low temperature retard the heat exchange, resulting the grown CNTs' morphology distorted, while water does overcome this shortcoming and the reactivity still remains high (Vittori Antisari *et al.*, 2003). Dissolving NaCl in the de-ionized water was later found enhancing the cooling ability and conductivity of the surrounding agent which was more suitable for SWCNTs production (Wang *et al.*, 2005).

EAD is an approach that grows CNTs at higher temperature as compared with other production methods. As a result, the wall perfection of CNTs from EAD are usually better and the yield per unit time also higher (Ajayan and Ebbesen, 1997).

### **2.2.2 Laser Ablation**

Smalley (1992) was the pioneer for applying laser ablation (LA) in the carbon world by developed LA equipped with annealing furnace. The apparatus setup is shown in Figure 2.4. The LA was first applied to overcome the shortcoming that poised by EAD for SWCNTs synthesis which likely to deteriorate. Smalley's group fruitfully produced SWCNTs by adding metal particles in the graphite just like EAD (Guo *et al.*, 1995). 1.2 % of cobalt/nickel with 98.8 % of graphite composite that placed in a quartz tube furnace at 1200°C under the argon atmosphere (~500 Torr ) was used by Smalley's group for the production of SWCNTs in 1996 (Thess *et al.*, 1996). The diameter distribution of SWCNTs obtained was in between 1.0-1.6 nm with purity of 90%. LA is a technique that laser with high energy density is utilized to vaporize carbon with very high boiling point and CNTs nucleated with catalyst. In LA, vapor plume that formed by catalyst and carbon expands and cools rapidly in laser pulse, SWCNTs are nucleated as the size of catalyst condense to a size that large enough. The growth will only stop when the catalyst particles become too large or coated by carbon layer (Scott *et al.*, 2001, Yudasaka *et al.*, 2002). The method has several advantages, such as high-quality SWCNT production, diameter control, and possible investigation of growth dynamic to the production of new materials

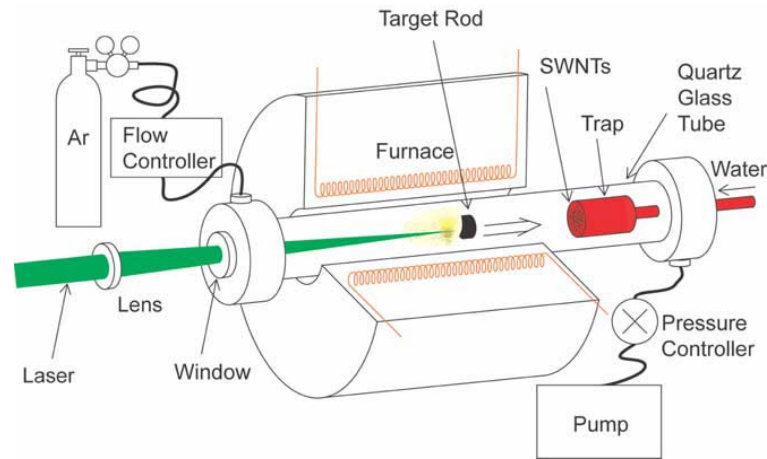


**Figure 2.4.** Schematic diagram of CNT formation apparatus by the laser ablation method (Ando et al., 2004)

For the synthesis of SWCNTs in LA, the catalyst has 3 criteria to fulfill during nucleation, which are good in graphitization, low solubility in carbon, and with a stable crystallographic orientation on graphite. NiCo, Ni, and NiFe are among the catalysts that fulfill these three conditions (Yudasaka *et al.*, 2002). Besides that, the laser used also plays the significant role in SWCNTs growth. Continuous wave laser provides more heat and higher evaporation rate of carbon for better yield of high quality SWCNTs as compared with pulse mode condition (Maser *et al.*, 2001). The higher the laser power will result SWCNTs with larger diameter, while bamboo-like CNTs favorable in low laser power (Zhang *et al.*, 2003a). The argon and nitrogen atmosphere was found to be most suitable for SWCNTs, instead helium only produce amorphous carbon (Maser *et al.*, 2001, Muñoz *et al.*, 1999). Meanwhile, the pressure between 200 and 400 Torr was the best for SWCNTs with maximum yield. Lower than this range promoted the formation of powdery-like soot material, while higher pressure will hinder the diffusion of carbon and catalyst plume and lower the yield (Muñoz *et al.*, 2000). LA is a continuous process that can be scaled up for mass production of SWCNTs with high quality and purity. However the cost of the laser photons is the main obstacle that prohibits the up scaling.

### 2.2.3 Flame synthesis

Flame synthesis is another method that is capable of producing CNTs. It involves the direct combustion of hydrocarbon in the presence of an oxidizer. The CNTs are normally grown directly on an alloy substrate, (Merchan-Merchan *et al.*, 2004) such as catalytic rod-like probes (Yuan *et al.*, 2003) grids or plates (Pan *et al.*, 2004).

Flame synthesis is a very energy-efficient process because the fuel itself is a source of heat and carbon. The temperature achieved can be as high as 1600 K, which is hard to achieve with CVD in a conventional furnace. For CNT synthesis over a large area, it is more economical to use multiple flames to achieve a controllable residence time and the desired flame region (Vander Wal, 2000). The production efficiency and yield per energy input is lower than that of CVD, making this method suitable for industrial production (Yuan *et al.*, 2002). Additionally, flame synthesis is a simple one-step method that without substrate preparation. However, complex substrate preparation has also been reported for flame synthesis (Li *et al.*, 2009, Li *et al.*, 2007). The growth mechanism of CNTs in the flame synthesis of hydrocarbon can be divided into 3 main steps (Arana *et al.*, 2005, Yuan *et al.*, 2002). First, the hydrocarbon fuel is pyrolysed in the preheated zone to form hydrocarbon species, which will be the carbon source for the CNTs, while the metal particles form on the surface of the alloy. The hydrocarbon species diffuse onto the catalyst at an appropriate temperature and is then absorbed by the catalyst to nucleate the growth of CNTs. Plate 2.1 shows the apparatus for flame synthesis.

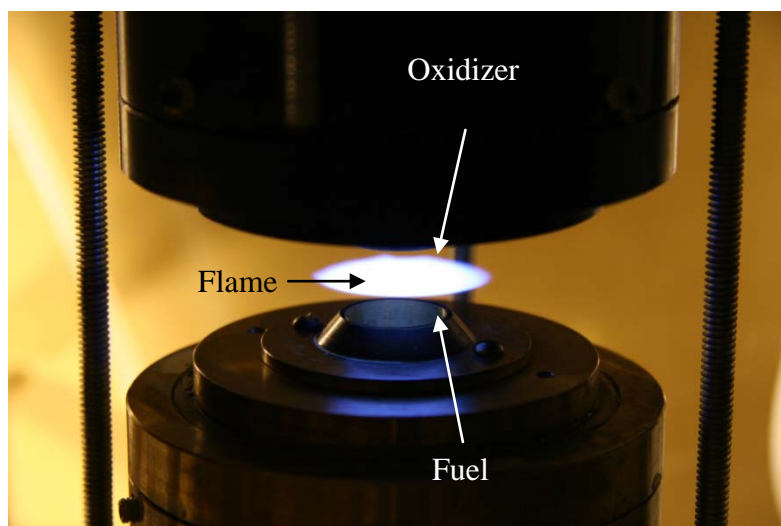


**Plate 2.1.** Image of the flame synthesis method, the white disc in the middle is the counterflow diffusion flame. (Tse, 2011).

There are two major flames used for CNTs synthesis, the most widely used is the simple concurrent diffusion flame, while the other counterflow diffusion flame (Merchan-Merchan *et al.*, 2006). Woo *et al.* (2004) reported that the formation of CNTs on a catalytic substrate occurred at a location outside of the sooting zone and the flame front of counterflow diffusion flame. Xu *et al.* (2006) confirmed this point by growing CNTs at the tip of the flame. However, the CNTs were shorter in length than those produced inside the flame. CNTs are commonly found in the sooting region of different kinds of catalytic probes used because of higher temperatures, which promote the formation of active catalytic nanoparticles for CNT nucleation. The studies of non-premixed diffusion flames show that the CNTs grow profusely in the area near to the centreline of the flames but not at the centre because the centre of the non-premixed feed is lacking in unsaturated carbon species and CO that will contribute to the formation of CNTs (Xu *et al.*, 2006).

Flame synthesis is a less popular method for CNTs synthesis. There are several shortcomings to this method. The apparatus for the flame synthesis, especially the burner, is complicated for the morphology of the flame to be controlled. The

gaseous fuels must be injected safely and carefully. The main drawback to this method is the poor quality of the CNTs obtained. From our review, the majority of the produced CNTs are not straight, except for those synthesized with the aid of an electric field. The bean-sprout-like bundles containing encapsulated particles at the tips of the nanotubes always are the main product, which limits the application in certain fields.

## **2.2.4 Catalytic Chemical Vapor Deposition**

Catalytic Chemical Vapor Deposition (CCVD) was first demonstrated by Yacaman *et al.* (1993) by decomposition of ethylene and iron oxide nanoparticles as catalyst. CCVD is now the most popular and most widely used technique for the growth of CNTs. As compared with LA and EAD, CCVD is a simple and economic technique for synthesizing CNTs at low temperature and ambient pressure, and better in crystallinity of the CNTs as compared with flame synthesis. Besides, it is very versatile. CNTs can be grown from various substrates to form CNTs in different form. Hydrocarbon whether in liquid, gaseous or solid state also can be applied as carbon source. CCVD is broadly studied and various advanced techniques were developed in order to improve the productivity of CCVD and reliability of the product. There are three other conventional CVD methods: hot-filament CVD (HF-CVD), plasma-enhanced CVD (PE-CVD), and floating catalyst CVD (FC-CVD).

### **2.2.4.1 Plasma enhanced chemical vapor deposition**

PE-CVD outclasses both simple CCVD and HF-CVD in terms of the alignment of the synthesized CNTs because of the bias applied to the substrate